Noise Characterization in Circular Dichroism Spectroscopy

JULIE M. DiNITTO and JOHN M. KENNEY*

Department of Physics, East Carolina University, Howell Science Complex, E. 10th Street, Greenville, North Carolina 27858-4353

Circular dichroism (CD), defined as the difference in absorption between left and right circularly polarized light, is used to spectroscopically study the structures of chiral materials. In this article, various methodologies are presented for characterizing the performance of CD spectrometers to determine (1) experimental conditions for optimal data collection, (2) noise characteristics dependent on machine parameters, (3) the relative significance of spectral data as a function of detector gain, and (4) stray light and dark current as a function of wavelength. The results of case studies of two commercial CD spectrometers (specifically, Jasco J810 and J815) are described. The analyses show that the variation of CD signal is Poisson distributed and hence can be considered shot noise. Also, optimum scan parameters are established and a weighting function of CD data significance is produced so that wavelength-dependent gain (as determined by the high tension, HT, voltage applied to the photomultiplier tube, PMT, detector) can be accommodated. Lastly, the amount of stray light and dark current for the photomultiplier tube is determined. Though specific to the Jasco CD spectrometers characterized in this study, it is expected that all CD spectrometers exhibit similar behavior and the methodology described here can be usefully applied to characterize CD spectrometers independent of manufacturer.

Index Headings: **Circular dichroism; Linear dichroism; Stray light; Dark current; Noise; Spectroscopy; High tension.**

INTRODUCTION

Circular dichroism (CD) spectroscopy is a technique designed to investigate the structure of chiral molecules, particularly biological ones.[1] In CD spectrometers the magnitude of a CD signal, ΔA_{CD}, usually measured in millidegrees (mdeg), is the difference in absorbance between right- and left-handed circularly polarized light as a function of wavelength as shown in Eq. 1:[2]

$$\Delta A_{CD}(\lambda) = A_L(\lambda) - A_R(\lambda) \tag{1}$$

When right-handed and left-handed light, produced by a photoelastic modulator (PEM), passes through a biological sample, the differential absorption due to the chiral molecular arrangement results in spectral features involving negative and positive peaks.[3] For example, in protein systems, peptide linkages exhibit spectral features in the far UV (amide) range (180–250 nm) that are associated with the secondary structures (e.g., alpha helices) and can detect small changes in these structures (e.g., increase in beta sheet due to a decrease in pH).[4] The advantage of using CD is to study molecular configurations and their dynamics at low protein concentration under physiological conditions in a near in vivo state. CD, therefore, is an important technique that complements X-ray crystallography and nuclear magnetic resonance by providing data on structures and dynamics under conditions not normally attainable by these techniques.

The validity of quantitative analysis (e.g., secondary structure prediction) of CD spectra depends on an accurate measure of the noise in the spectra. A systematic study of the signal-to-noise ratio (SNR), particularly as a function of wavelength or detector gain, in CD spectroscopy has not been previously published. The research presented here addresses this need, detailing an investigation of the SNR as a function of wavelength and machine parameters for two commercial CD spectrometers (Jasco J810 and J815). The theoretical prediction of the SNR is tested through the ratio of the signal-to-noise ratios (RSNR) under various experimental conditions. Finally, this study provides a methodology that may prove useful for characterizing spectrometers in general.

The amount of noise depends on the light intensity (photon flux). Peculiar to CD (and linear dichroism, LD) spectroscopy, the output DC voltage (v) of the detector is held constant in order to remove the effect of a variation (as a function of time and wavelength) in the photon flux (I_0) incident on the PMT. PMT gain and I_0 are reciprocally related. For example, if I_0 increases, the gain of the PMT decreases concomitantly so that the measured CD signal is independent of I_0. This is only true as long as the absorbance due to chirality (CD) is much less than the total absorbance (e.g., <1 in 100).[5] The variation in the detected photon flux is shot noise. Shot noise is expected to follow a Poisson distribution[6] and hence is related to the reciprocal of the gain so that the lower the gain (a consequence of a lower voltage, HT, applied to the PMT) the higher the SNR.

As in most electronics, major sources of noise in CD spectroscopy include interference, Johnson (thermal) noise, systematic noise, flicker noise, and shot noise. Interference and Johnson noise are mitigated by careful instrument design and maintenance of constant operating conditions (e.g., temperature). Flicker noise ($1/f$ noise) is insignificant in CD spectroscopy because the signal is generated at approximately 50 kHz. In CD spectroscopy a lock-in amplifier is employed to filter out contributions other than those at the PEM oscillation frequency and phase, although a small amount of linear dichroism may "leak" through.[7,8] Therefore, shot noise is the dominant source of noise.

In this article, shot noise is characterized by using the SNR. The SNR depends on the brightness of the light source, efficiency of the spectrometer, absorption of the sample, and efficiency of the detector (PMT), all of which are wavelength dependent. Noise in the PMT is specifically discussed. The SNR is also a function of experimental parameters: bandwidth, slit width, scan speed, response time (RT), and number of averaged scans, all of which affect the number of photons contributing to the signal. The SNR as a function of these parameters is described theoretically and determined experimentally.

Received 19 July 2011; accepted 1 November 2011.
* Author to whom correspondence should be sent. E-mail: kenneyj@ecu.edu.
DOI: 10.1366/11-06417

SHOT NOISE AND POISSON STATISTICS

The signal detected (current output from the PMT) in CD spectroscopy is directly proportional to the number of photons n entering the detector. Consequently, according to the Poisson distribution, the signal-to-noise ratio (SNR) can be defined as

$$SNR = \frac{n}{\sqrt{n}} = \sqrt{n} \tag{2}$$

In CD spectroscopy, single photon counting is not normally possible, because the PMT gain varies to maintain a constant output and the photon flux is very high.[9] Therefore, an indirect approach is taken to theoretically calculate and experimentally measure the noise. The SNR (as a function of photon count) can be indirectly calculated by taking the ratio of two SNRs, thus, removing the signal, leaving only the ratio of the noise. The theoretical (calculated) RSNR is defined as,

$$RSNR = \frac{SNR_{1n}}{SNR_{2m}} = \frac{n}{\sqrt{n}}\frac{\sqrt{m}}{m} = \sqrt{n}\frac{1}{\sqrt{m}} = \frac{\sqrt{n}}{\sqrt{m}} \tag{3}$$

where m and n are measures of the number of photons.

The same indirect approach is also used to experimentally measure the RSNR. The experimental SNR is given by:

$$SNR = \frac{S}{N} = \frac{\Delta A_{CD}(\lambda_i)}{\sigma(\lambda_i)} \tag{4}$$

where the $\Delta A_{CD}(\lambda_i)$ is the average of the signal at a specific wavelength and the noise is the standard deviation, $\sigma(\lambda_i)$, of $\Delta A_{CD}(\lambda_i)$. Similar to the theoretical representation of the SNR, the CD signal will be the same for every experiment, but the noise, of which $\sigma(\lambda_i)$ is a measure, varies. The experimental RSNR can be defined as:

$$RSNR(\lambda_i) = \frac{SNR_1(\lambda_i)}{SNR_2(\lambda_i)} = \frac{\sigma_2(\lambda_i)}{\sigma_1(\lambda_i)} \tag{5}$$

where the experimental noise is the standard deviation of the CD signal (in mdeg). Hence the relationship between the experimental and theoretical determination of the photon count and noise is given by:

$$RSNR(\lambda_i) = \frac{\sqrt{n}}{\sqrt{m}} = \frac{\sigma_2(\lambda_i)}{\sigma_1(\lambda_i)} \tag{6}$$

and is a test of the hypothesis that the noise is Poisson distributed shot noise.

DARK CURRENT AND STRAY LIGHT

The DC voltage, v (the time average signal from the PMT) can be written as the product of two gains and the sum of three cathode currents:

$$v(\lambda_i) = G_{I/V} G_{PM}[V](j_p + j_s + j_d) \tag{7}$$

where $G_{I/V}$ is the gain of the current-to-voltage converter for the PMT, $G_{PM}[V]$ is the relative gain provided by the Jasco company (relationship between the gain and HT of the PMT), and the three currents that represent the cathode current are due to the primary light beam (j_p), stray light (j_s), and dark current (j_d). Under normal operation of the CD spectrophotometer, HT on the PMT (V_{0f}) is adjusted to maintain a constant time average DC output (v_{0f}).[8] Under exceptional conditions when there is too little light, the V_{0f} limit is met; hence v_{0f} is no longer constant and begins to decrease. Therefore, measuring the gain on the PMT as well as the DC output as a function of wavelength allows the fraction ($v_{fraction}$) of light due to dark current and stray light:

$$v_{fraction} = \frac{v_f G_{PM}[V_0]}{v_0 G_{PM}[V_f]} \tag{8}$$

where V_0 and v_0 are the HT and DC signal under normal operating conditions and V_f and v_f are the HT and DC under exceptional conditions. The subscript f indicates the presence of a cutoff filter. Using a cutoff filter allows the stray light and dark current contribution to be separated from the main contribution of the signal. Likewise, to separate the stray light from the dark current, the PMT window is blocked and V_f and v_f are replaced by V_{dark} and v_{dark}.

PHOTOMULTIPLIER TUBE DETECTOR

An ideal PMT has a number of dynodes p with a dynode voltage V_d that is equal across every dynode. The HT voltage, V_0, applied to the PMT is equally divided by a voltage divider and the voltage at each dynode is:

$$V_d = \frac{V_0}{p+2} \tag{9}$$

where V_0 is the total voltage applied to the PMT and p is the number of dynodes in the PMT. The "+2" includes the potential drop between the cathode and first dynode and the anode and last dynode. The gain of each dynode is the number of secondary electrons per primary electron and can be defined as

$$G_{d_i} = kV_{d_i} \tag{10}$$

where k is the number of electrons produced per volt of electric potential across a single dynode assuming the material and geometry of the dynodes are identical. For the ideal PMT described, the V_{d_i} are equal and hence the G_{d_i} are equal so that the total gain G_{PM} of the PMT would be

$$G_{PM} = (G_{d_i})^p = (kV_{d_i})^p \tag{11}$$

Substituting in Eq. 9:

$$G_{PM} = \frac{k^p}{(p+2)^p}(V_0)^p \tag{12}$$

and hence,

$$\ln(G_{PM}) = p\ln\left(\frac{k}{p+2}\right) + p\ln(V_0) \tag{13}$$

which provides a linear relationship between the natural log of the gain and the natural log of the applied voltage, V_0 (see Fig. 5). In practice, however, the photomultiplier tube (Hamamatsu R376 in the Jasco J810 and J815) does not behave perfectly as the ideal case described (Fig. 5). Instead, the slope of the line is nearly, but not exactly, equal to the number of dynodes p. In any case, the slope appears to be proportional to the number of dynodes. This is consistent with the specification (calibration)

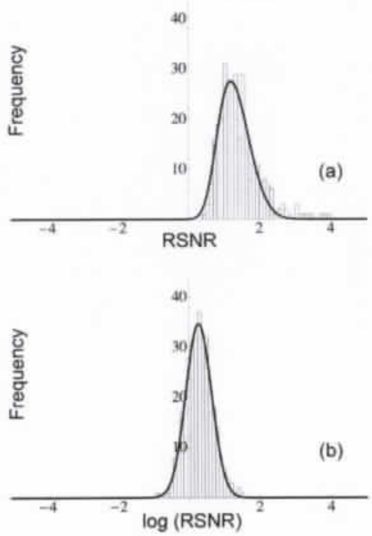

FIG. 1. Histogram log transformation for 1 vs. 2 second response time.

supplied by the manufacturer and implies that the methodology is correct.

EXPERIMENTAL: MATERIALS AND METHODS

All CD spectra were collected using a Jasco J810 and a J815 spectrometer equipped with the Jasco Instrument Driver Version 1.19 and Spectra Manager 1.53E.[10] Four different experiments, each varying a different single parameter, were executed. In each experiment a Hellma Suprasil quartz cell of path length 1 mm was used. The parameters for all the experiments (except for the parameter being tested) were: a single scan (1 accumulation), response time (2 s), scan speed (200 nm/min), and bandwidth (2 nm), unless otherwise noted in the experiment. These particular parameters were chosen to show the effect on the SNR of the upper limit of the parameter values recommended by the Jasco Inc instrument manual.[10] All experiments were repeated on different days with the same results.

The first experiment explored the effect that the number of scans used to make an average had on the RSNR. Forty sets of spectra were recorded for a camphorsulfonic acid (Sigma Aldrich) solution (0.06 mg/mL) with scanning wavelength ranges 180–350 nm, 350–500 nm, and 500–700 nm. The number of scans averaged ranged from 1 scan to 4 scans.

The second experiment examined the effects of scan speed and response time. Ten individual spectra, each consisting of a

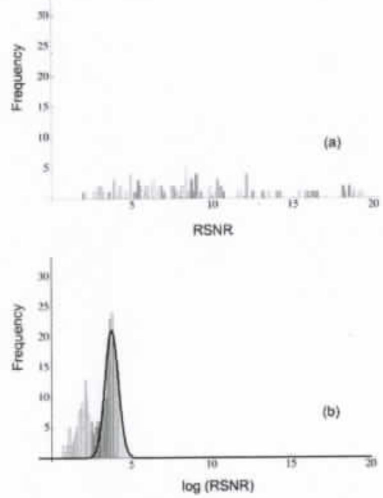

FIG. 2. Histogram log transformation for 1 vs. 8 nm bandwidth.

single scan, were recorded for distilled water with various scan speeds and response times (see Table I), over the wavelength range 180–500 nm. The RSNR was found to be independent of scan speed; therefore, the scan speed was set appropriately for the response time as per the Jasco user manual recommendation.

The third experiment considered the effect of bandwidth. The width of the CD monochromator slit (measured in μm) continuously changes to maintain a constant bandwidth. Ten single scans of distilled water at bandwidths of 1, 2, 4, and 8 nm were collected over wavelength range 180–700 nm.[†]

The fourth experiment tested the effect of the slit width. The width of the slit was held constant over the whole spectrum; therefore, the bandwidth (which is wavelength dependent) varied. In the slit-width experiment, ten individual scans of distilled water over wavelength range 700–180 nm, at slit widths of 100, 500, and 1000 μm, were recorded. For the Jasco J810 and J815, roughly 1 nm of bandwidth corresponds to 1 mm of slit width in the UV and 1 nm to 10 μm in the visible light region. Parameters held constant were response time (1 s) and scan speed (200 nm/min).

To test the dark current and stray light for the PMT, a 1 mm water sample was placed in the sample chamber of the CD

[†] When bandwidth is varied, not only is the exit slit changed to the specified bandwidth, but also the slits in the double monochromator vary in the same manner. Therefore, the number of photons depends on the square of the bandwidth.

TABLE I. Chosen parameters for response time and corresponding scan speed.

Response time (s)	Scan speed (nm/min)	Scan speed (max) (nm/min)
0.25	1000	–
0.5	500	1000
1	200	500
2	100	200
4	50	100
8	–	50

spectrometer and values for V_0 and v_0 were recorded over wavelength range 170 to 400 nm every 10 nm and every 2 nm between 190 nm and 170 nm. Water was chosen because it is opaque in the far UV (<170 nm) and the machine parameters were chosen from an analysis of the previous experiment (see analysis).[11] Two other similar experiments were performed, one with a 300 nm cutoff filter (to measure V_f and v_f) provided by Jasco and the other with a shuttered PMT window (to measure V_{dark} and v_{dark}). All instrument parameters were the same for the two experiments.

ANALYSIS

For a large number of photons,[12] a normal distribution is a good approximation to a Poisson distribution; hence, for each RSNR a histogram was constructed and fit to a skewed[‡] normal distribution (see Figs. 1a and 2a). Then the data was log transformed in order to determine accurately the averaged RSNR and to remove any Cauchy effects for a more robust analysis (see Figs. 1b and 2b).[13,14] Through partition analysis of the RSNR (by recursive partitioning and decision tree analysis),[15] it was observed that at higher wavelength ranges, the bandwidth-dependent RSNR does not always strictly follow a Poisson distribution (see Fig. 2b). Furthermore, there was some deviation from linearity in the higher wavelength ranges (480–700 nm) on the J810 for the bandwidth-dependent RSNR. Data collected on the J815 did not display an apparent bandwidth-dependent RSNR nonlinearity, but of all the experimentally tested parameters it suffered the largest deviation. Even so, the RSNR analysis shows that in general J815 behaves similarly to the J810. Table II indicates ranges and tests, principally at long wavelengths and narrow bandwidths, that exhibit the largest divergence between the RSNR predicted by Poisson statistics and the RSNR determined experimentally. The results for the J810 showed a larger divergence than for the J815. These results suggest that in these ranges the noise in the CD signal cannot be predicted solely by Poisson statistics and hence may be complicated by systematic error. Table III indicates that over more ranges and tests many of the experimental results exhibit Poisson distributions, but specific ones exhibit some divergence between predicted and determined RSNRs. Again, the divergence was larger for the J810 results. The results of other ranges and parameters, particularly response time and averaged number of scans, demonstrated experimentally determined RSNRs that follow Poisson statistics and coincided with theoretical predictions.

Scan speed does not affect the RSNR, in accordance with

[‡] Data is skewed, because the magnitude of the signal (number of photons) can never be less than zero.

TABLE II. Data collected in ranges where the RSNR is not normally distributed.

Parameter	Range (nm)	Test
Jasco J810		
Bandwidth	480–700	1 vs. 2 nm
Bandwidth	480–700	1 vs. 4 nm
Bandwidth	480–700	1 vs. 8 nm
Bandwidth	480–700	2 vs. 4 nm
Bandwidth	480–700	2 vs. 8 nm
Jasco J815		
Parameter	Range (nm)	Test
Bandwidth	180–480	1 vs. 4 nm
Bandwidth	480–700	1 vs. 4 nm
Bandwidth	480–700	1 vs. 8 nm
Bandwidth	480–700	2 vs. 4 nm
Bandwidth	480–700	2 vs. 8 nm

machine design, but it can affect the shape of the signal. If the scanning speed is too fast for the response time used, a sharp peak in the spectra will be broadened. On the other hand, as the response time increases, the number of photons that are collected increases and therefore the SNR increases, i.e., σ decreases for the same CD signal value (see Fig. 3). This is similar to the experiment in which the number of scans averaged is varied (Fig. 4). This is consistent with the aforementioned coincidence between predicted and determined RSNR based on response time and number of scans averaged.

The RSNR analysis depends on a well-calibrated PMT in which the relationship between gain and detector HT voltage, V_0, is known. Therefore, experiments were performed to calibrate the PMT and it was observed that the PMT responds as expected based on the manufacturer specifications (Fig. 5). All slopes from the data collected on the Jasco J810, the Jasco J815, and the information provided by Hamamatsu are similar:

$$\text{Amplification} = 7.44 \times \text{Sample Voltage} - 15.7_{\text{R376 Hamamatsu}}$$

$$\ln(\sigma^2) = 6.4(3) \times \ln(V_0) - 17.4(7)_{\text{Jasco J815}}$$

$$\ln(\sigma^2) = 7.5(6) \times \ln(V_0) - 20(1)_{\text{Jasco J810}}$$

TABLE III. Data collected on Jasco J810 and J815 parameters that are the least linearly behaved.

Parameter	Range (nm)	Test
Jasco J810		
Bandwidth	180–480	1 vs. 4 nm
Bandwidth	480–700	4 vs. 8 nm
Slitwidth	180–500	100 vs. 500 um
Slitwidth	180–500	100 vs. 1000 um
Slitwidth	500–700	100 vs. 500 um
Slitwidth	500–700	100 vs. 1000 um
Slitwidth	500–700	500 vs. 1000 um
Averaged Scans	500–700	1 vs. 4 averaged scans
Jasco J815		
Parameter	Range (nm)	Test
Bandwidth	480–700	1 vs. 2 nm
Bandwidth	480–700	4 vs. 8 nm
Slitwidth	500–700	500 vs. 1000 um

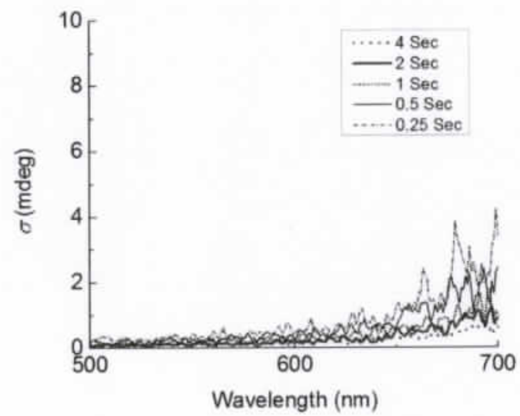

FIG. 3. σ vs. wavelength for response time.

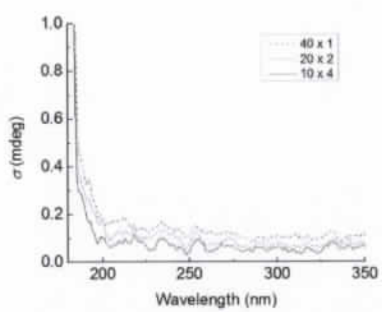

FIG. 4. σ vs. wavelength for averaged number of scans. 40 total scans averaging 1, 2, and 4 scans for variation.

The first equation was derived from data provided by Hamamatsu,[8] the second is the average of all data collected on the Jasco J815, and the third is the average of all the data collected on the Jasco J810. Therefore, the PMT in both J810 and J815 responds as described by Hamamatsu's current amplification characteristics. It appears that the voltage divider is not acting in the ideal case as described in the Photomultiplier Tube section, so that the number of dynodes predicted by theory is not exactly the same as the number determined by experiment. Therefore, though the PMT cannot be modeled simply as an equipartition of detector HT voltage across all the dynodes, its voltage-gain performance is calibrated and is similar to that provided by the PMT manufacturer.

Table IV and Fig. 6 show how SNR depends on gain. The amount of noise varies with wavelength because the gain (as determined by HT) varies. Gain is not a simple function of wavelength; however, gain is a well understood function of HT. Therefore, the HT (which is usually recorded with the CD signal) is required in order to determine the relative SNR at different wavelengths. The HT is therefore useful in determining the significance of the CD data as a function of SNR. For example, in CD studies of protein binding or unfolding, data is sometimes only analyzed at a single wavelength to calculate a titration plot. This ignores all the other data in the spectrum. Therefore, to improve the accuracy of the titration, the data is integrated over wavelength. Often, however, data across the entire spectrum is treated with equal weight even though the CD signal at different wavelengths exhibits very different noise characteristics (i.e., different SNRs); that is, the data are combined regardless of their significance. Using a weighting function (by HT, a measure of gain) the data can be more appropriately integrated over a broad spectrum. The experimentally determined relative SNR as a function of HT for the J810 and J815 data is shown in Fig. 6. It can be used to quantifiably weigh data by their SNR-dependent significance determined by HT.

Optimal data collection also depends on machine parameters. The parameters affect the shot noise and systematic noise (e.g., baseline drift) in opposing ways. For example, lengthening the response time includes more photons, thereby increasing the SNR; however, this requires a longer time to complete a spectrum, thereby increasing the effect of drift and mitigating any shot-noise reduction benefit. In this study the J810 and J815 were optimal for scans with a 1–4 s response time at a 50–200 nm/min scan speed and a 1–8 nm bandwidth.

[8] *R376 Photomultiplier Tube* (Hamamatsu Corporation, Middlesex, NJ, 08846), Tel. (201) 469-6640.

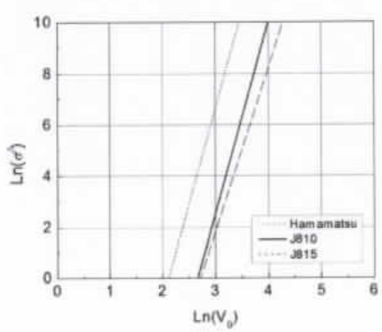

FIG. 5. Ln of σ^2 vs. ln of the gain for Hamamatsu R376 connected to Jasco J810, Jasco J815, and data from Hamamatsu. Dotted line is data from Hamamatsu, solid line is Jasco J810, dashed line is Jasco J815.

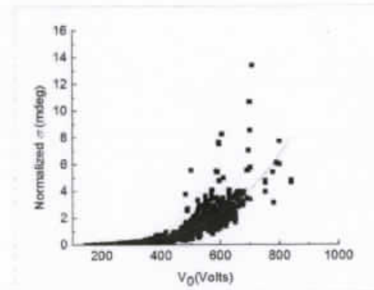

FIG. 6. Relative σ vs. V_0 for data collected on J810 and J815. $R = 0.801$. $\sigma = 1.8(1) \times 10^{-10}\ HT^{[illegible]}$.

TABLE IV. Look-up table for Fig. 6.

HT (Volts)	σ (mdeg)	HT (Volts)	σ (mdeg)	HT (Volts)	σ (mdeg)
100	0.003	300	0.177	500	1.129
120	0.006	320	0.223	520	1.301
140	0.011	340	0.278	540	1.492
160	0.018	360	0.342	560	1.703
180	0.028	380	0.417	580	1.934
200	0.041	400	0.502	600	2.188
220	0.057	420	0.599	620	2.464
240	0.079	440	0.71	640	2.765
260	0.105	460	0.834	660	3.092
280	0.138	480	0.973	680	3.446

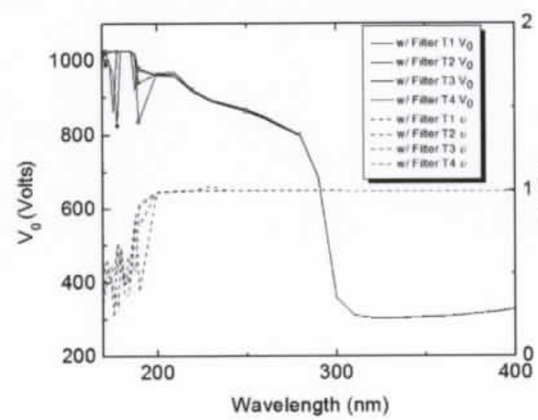

FIG. 7. V_0 and υ for Hamamatsu R376 PMT on Jasco J810.

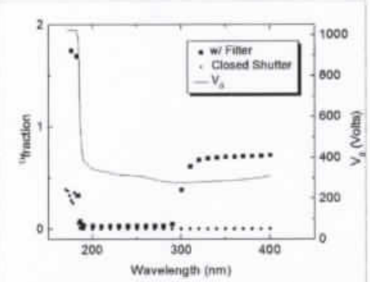

FIG. 8. Dark current and stray light for Hamamatsu R376 PMT on Jasco J810.

The largest bandwidth used should be consistent with the width of the spectral features. It was also found that the SNR rose sharply when HT exceeded 400 volts; therefore, the CD signal at this high HT was considerably less significant and for the benefit of quantitative analysis involving the integration of data over a range of HT the data should be appropriately weighed using Fig. 6 and Table IV.

Stray light and dark current can degrade the signal. A single cutoff filter (300 nm) was used to determine stray light and dark current effects. In this experiment, the HT reaches a saturation point and the DC voltage begins to decrease.* This was repeated under multiple trials with the same filter and the results are shown in Fig. 7. Applying Eq. 8 to this data, the ν fraction of stray light and dark current can be determined. Figure 8 is a graph of the ν fraction and V_0. Between 290 nm and 184 nm the amount of stray light is about 3.0(1)% and dark current is about 0.1(1)%. Between 190 nm and 170 nm V_0 has reached its saturation point and the stray light dominates and dark current is a small but measurable contribution [ν = 0.32(1)]. Therefore, under exceptional conditions (V_0 approaching 900 volts), stray light and dark current dominate the signal. On the other hand, under normal conditions ($V_0 <$ 800 volts) stray light and dark current are of little consequence.

CONCLUSION

The hypothesis that the noise associated with the variation of CD signal is governed by Poisson statistics and therefore is shot noise was tested by studying the effects of various parameters (number of scans, bandwidth, slit width, and response time) on the SNR for the Jasco CD spectrometers (J810 and J815) over a wide wavelength range (180–700 nm). The hypothesis was confirmed for all of the parameters tested with a few notable exceptions at long wavelengths.

Bandwidth-dependent SNR begins to deviate from a Poisson distribution in the wavelength range between 480 and 700 nm and that deviation increases as bandwidth decreases. The deviation may be the result of the baseline drift, which is more pronounced at longer wavelengths. Also, there was some variation from the expected RSNR (yet still Poisson distributed) in certain wavelength ranges. For the CD monochromator, the width of the slits varies with wavelength to compensate for the wavelength-dependent dispersion to maintain a constant bandwidth over the wavelength range. Some slight misalignment of the slits that is exacerbated at longer wavelengths may produce the observed deviation. It is worth noting that in this regard the J815 performed better than the J810. This is an issue for studies using the longer wavelength range of the CD spectrometer, e.g., metal-ion binding, which exhibits d–d CD peaks in the visible range.[16] This is not an issue for the majority of the CD spectroscopy of biological systems for which the secondary structure is of interest, because spectral features of secondary structures are in the far UV (the amide region) and the absorption due to side chains of proteins is in the near UV (the aromatic region). The SNR associated with the number of scans followed a Poisson distribution without exception; however, time-dependent systematic uncertainty or error (e.g., drift) poses the same problem as it does for the bandwidth and slit width experiments. The conclusion is that, as expected, the signal produced by the Jasco CD machines follows, with exceptions noted, a Poisson distribution over a broad range of parameters and hence is quantitatively predictable shot noise.

Under normal data collection conditions, effects of dark current and stray light in the UV range (<300 nm) were minimal until the HT detector voltage, V_0, begins to saturate (V_0 > 900 volts). After saturation occurs, the signal is dominated by stray light and dark current. It is worth noting that stray light and dark current provided insufficient "signal" to maintain a V_0 that was not saturated and hence under normal operating conditions ($V_0 <$ 600 volts) does not produce a false signal. Another important result of this study is the determination of the functional dependence of the significance (as measured by the relative SNR) of the spectral data on the detector voltage (V_0, a measure of gain). Thus, the variation over wavelength with respect to V_0 (see Table IV and Fig. 6) can be used to weigh the signal appropriately as a function of the significance (i.e., the SNR). This is expected to have an impact on experimental analyses that depend on combining or integrating data over a range of wavelengths for which there is a significant variation in V_0, for example in the low (<200 nm) wavelength and high (>500 nm) ranges where the HT is rising.

It is hoped that the results of this study will provide a useful guide for choosing parameters that optimize the use of modern Jasco CD spectrometers (namely the J810 and J815) as well as to provide a methodology for optimizing spectrometers in general. Furthermore, this study presents a mechanism for weighing spectral data appropriate to their significance (their SNR), using the HT detector voltage (via a lookup table and graph), thus allowing an accurate integration of the data over any spectral range.

ACKNOWLEDGMENTS

Appreciation is expressed to Dr. John C. Sutherland for advice on experimental techniques and to Dr. Anthony Kennedy for comments on the article.

* The absorption spectrum of the cutoff filter indicates that there is no appreciable fluorescence contribution (data not shown).

1. A. Rodgers and B. Nordén, *Circular Dichroism and Linear Dichroism* (Oxford University, New York, 1997), 1st ed., p. 15.
2. A. Rodgers and B. Nordén, *Circular Dichroism and Linear Dichroism* (Oxford University, New York, 1997), 1st ed., pp. 6–7.
3. A. Rodgers and B. Nordén, *Circular Dichroism and Linear Dichroism* (Oxford University, New York, 1997), 1st ed., pp.16–32.
4. C. Dicko, F. Vollrath, and J. Kenney, Biomacromolecules **5**, 704(2004).
5. J. Sutherland, *Errors in Dichroic Spectroscopies Due to Large Signals or Improper Modulator Amplitudes* (CD2011 International Conference, Oxford, UK, July 25, 2011).
6. M. Fox, *Quantum Optics* (Oxford University Press, New York, 2006) pp. 76–82
7. Y. Shindo and Y. Ohmi, J. Am. Chem. Soc. **107**, 91 (1985).
8. B. A. Wallace and R. W. Janes, *Modern Techniques for Circular Dichroism and Sychrotron Radiation Ciracular Dichroism Spectroscopy: Volume 1 Advances in Biomedical Spectroscopy* (IOS Press, Amsterdam, 2009), 1st ed., p.19–72.
9. W. Becker, *Advanced Time-Correlated Single Photon Counting Techniques* (Springer, New York, 2005), 1st ed.
10. *Model J-810 Spectropolarimeter: Operation Manual* (Jasco Corporation, Baltimore, MD, 1999).
11. L. Robinson Painter, R. N. Hamm, E.T. Arakawa, and R. D. Birkhoff, Phys. Rev. Lett. **21**, 282 (1968).
12. J. R. Taylor, *An Introduction to Error Analysis* (University Science Books, Sausalito, CA, 1997), 2nd ed., pp. 250–251.
13. L. Breiman, J. Friedman, C. J. Stone, and R. A. Olshen, *Classification and Regression Trees* (Chapman and Hall/CRC, Boca Raton, FL, 1998).
14. O. Schabenberger and C. A. Gotway, *Statistical Methods for Spatial Data Analysis* (Chapman and Hall/CRC, Boca Raton, FL, 2005), 1st ed., pp. 271–273.
15. F. E. Harrell, *Regression Modeling Strategies* (Springer-Verlag, New York, 2001), Corrected Ed., pp. 26–27.
16. J. B. Pollock, P. J. Cutler, J. M. Kenney, P. J. Gemperline, and C. S. Burns, Anal. Biochem. **377**, 223 (2008).